IOPscience iopscience.iop.org

Home Search Collections Journals About Contact us My IOPscience

Magnetic studies of multiferroic $Bi_{1-x}Sm_xFeO_3$ ceramics synthesized by mechanical activation assisted processes

This article has been downloaded from IOPscience. Please scroll down to see the full text article.

2009 J. Phys.: Condens. Matter 21 026007

(http://iopscience.iop.org/0953-8984/21/2/026007)

View the table of contents for this issue, or go to the journal homepage for more

Download details:
IP Address: 129.252.86.83
The article was downloaded on 29/05/2010 at 17:04

Please note that terms and conditions apply.

J. Phys.: Condens. Matter **21** (2009) 026007 (6pp) doi:10.1088/0953-8984/21/2/026007

Magnetic studies of multiferroic $Bi_{1-x}Sm_xFeO_3$ ceramics synthesized by mechanical activation assisted processes

Deepam Maurya[1], Harikishan Thota[1], Ashish Garg[1,3], Brajesh Pandey[2], Prem Chand[2] and H C Verma[2]

[1] Department of Materials and Metallurgical Engineering, Indian Institute of Technology Kanpur, Kanpur 208016, India
[2] Department of Physics, Indian Institute of Technology Kanpur, Kanpur 208016, India

E-mail: ashishg@iitk.ac.in

Received 7 July 2008, in final form 14 October 2008
Published 9 December 2008
Online at stacks.iop.org/JPhysCM/21/026007

Abstract

$Bi_{1-x}Sm_xFeO_3$ ($x = 0.0$–0.2) ceramic samples were prepared by mechanical activation assisted solid-state-reaction synthesis. A stoichiometric mixture of Bi_2O_3, Sm_2O_3, and Fe_2O_3 powders was mechanically milled and this was followed by heat treatment at 700 °C for 1 h. Room temperature x-ray diffraction patterns confirmed the formation of perovskite structured $Bi_{1-x}Sm_xFeO_3$ phase. Vibrating sample magnetometry measurements showed that to a certain extent, Sm doping of $BiFeO_3$ leads to increased magnetization and a sharp magnetic transition at ∼380 °C. Mössbauer spectroscopy confirmed the presence of single-phase material for the doped compositions whereas electron paramagnetic resonance analysis showed the effect of doping on the variation in the degree of canting in the samples. At doping levels of 10 at.% Sm, the improvement in the magnetic behaviour appears to arise from a combination of the propensity of the samples to form pure phase material, partial destruction of spin cycloids, increased canting of spins and interaction between magnetic ions.

(Some figures in this article are in colour only in the electronic version)

1. Introduction

In general, multiferroics exhibit at least two of the four ferroic properties: ferroelasticity, ferroelectricity, ferromagnetism and (recently found) ferrotoroidicity [1–3]. $BiFeO_3$ (BFO) is a multiferroic material in which ferroelectricity and antiferromagnetism coexist at room temperature [4, 5]. It exhibits two types of long-range ordering: the *G*-type collinear antiferromagnetic ordering below a Néel temperature (T_N) of 643 K and the ferroelectric ordering below 1103 K [6, 7]. The compound has a distorted ABO_3 perovskite structure with the rhombohedral space group $R3c$ [8, 9]. Bulk BFO shows a spiral magnetic spin cycloid with a periodicity of ∼620 Å [10] and as a result no macroscopic magnetization is measured [11]. However, canting of spins may lead to residual magnetic moment [12]. To suppress the spiral structure, a few solutions have been proposed such as application of high magnetic fields ($H_c \sim 20$ T) [11], use of thin film samples with a strong substrate induced anisotropy [13], substitution of Bi ions by rare earth ions (e.g. Sm, Dy, La, Gd) [14] or, in the form of solid solutions, with compounds such as $PbTiO_3$ and $BaTiO_3$ [15, 16]. Among doped samples, previous studies on A-site doping with Sm^{3+} and Pr^{3+}, both isovalent lanthanide ions, have been reported to result in an increased remnant magnetization of BFO [17–19]. In addition, B-site substitution (of Fe^{3+}) by a variety of ions (e.g. Co, Mn, Nb etc) is shown to result in improved magnetic behaviour of this material [20–24]. In another study, A-site (Bi^{3+}) substitution by a non-magnetic ion such as Ba^{2+} in BFO has been shown to enlarge the degree of distortion [25], which in turn leads to spontaneous magnetization.

In this paper, we report detailed magnetic characterization of $Bi_{1-x}Sm_xFeO_3$ ($x = 0.0, 0.1, 0.2$; named BFO, BSFO-1, BSFO-2, respectively) ceramics prepared by a

[3] Author to whom any correspondence should be addressed.

 © 2009 IOP Publishing Ltd Printed in the UK

mechanical activation assisted method. In addition to using structural characterization, we have used vibrating sample magnetometry, Mössbauer spectroscopy and electron paramagnetic resonance to achieve a detailed understanding of the magnetic behaviour of these ceramics. Barring a few reports [26, 27], not much work has been done on the Mössbauer spectroscopy and electron paramagnetic resonance of multiferroic ceramics.

2. Experimental details

Stoichiometric amounts of Bi_2O_3, Sm_2O_3 and Fe_2O_3 (purity ∼99.9%) were mixed and subsequently milled in a high energy planetary ball mill using a balls to powder ratio of 1:1 for a period of 100 h. The milled $Bi_{1-x}Sm_xFeO_3$ mixture was further calcined at 700 °C for 1 h in air followed by furnace cooling.

Phase identification was performed with an x-ray diffractometer (Siefert, Model: ISO Bebyeflex 2002) using Cu Kα radiation. Magnetic measurements were made using a vibrating sample magnetometer (VSM; ADE Technologies, USA, Model: EV-7VSM). The sensitivity of the instrument is 10^{-6} emu. Mössbauer spectroscopy measurements were performed by using ^{57}Co as the radioactive source and a standard constant acceleration spectrometer. The magnetic resonance spectra were recorded with an EPR spectrometer (Brucker EMX X-band). The samples were rolled into cylindrical shapes by wrapping them in Teflon tapes. These samples were stuffed into a 4 mm diameter quartz capillary. The sample was placed at the centre of the resonant cavity placed between pole caps of an electromagnet. The magnetic field was scanned from 0–8000 G, while the resonance frequency (9.79 GHz) of the sample cavity was locked. The magnetic field was modulated at 100 kHz to detect the first derivative of the magnetic resonance absorption signal of the sample.

3. Results and discussion

3.1. X-ray diffraction

Figure 1 shows the x-ray diffraction (XRD) patterns of the 100 h mechanically activated and subsequently heat treated $Bi_{1-x}Sm_xFeO_3$ samples. The featureless nature of the uncalcined samples (the three patterns at the bottom) suggests amorphization of the samples after 100 h of mechanical milling of stoichiometric mixtures of Fe_2O_3, Bi_2O_3 and Sm_2O_3 powders. Mechanically activated samples were subsequently subjected to heat treatment at various temperatures. Peak matching with a standard BFO pattern suggested the formation of perovskite structured $Bi_{1-x}Sm_xFeO_3$ phase at 700 °C. The top three patterns in figure 1 show the XRD patterns of the samples calcined at 700 °C for 1 h. The main peaks, marked by asterisks (*), for the BFO sample match well with the standard BFO peak positions with Cu Kα radiation (ICCD file No. 74-2493). One may be tempted to assign some of the humps in the background of the spectra to the formation of secondary phases (such as one depicted by $) which cannot be ruled out from the XRD patterns alone. The phases that can form in competition to pure BFO, as inferred from the phase diagram, are $Bi_{25}FeO_{39}$ and $Bi_2Fe_4O_9$ which have been well studied by crystallographic and other techniques [28, 29]. However, as shown in later sections, further measurements with Mössbauer spectroscopy provide some more information on this. Apart from this, Sm-doped samples also showed peak broadening, although the peak positions remained the same. In solid-state-reaction processed samples, BFO phase is normally formed at temperatures above 825 °C [18]. The present work shows the formation of this phase at 700 °C, much lower than the previous reports, attributed to the increased defect density in the samples due to mechanical milling prior to calcination and hence enhancing the diffusibility of the species for phase formation. Previous reports related to the synthesis of various perovskite structures have also shown that mechanical activation assisted solid-state-reaction process decreases the synthesis or phase formation temperature and also overcomes the microstructural problems [30–34].

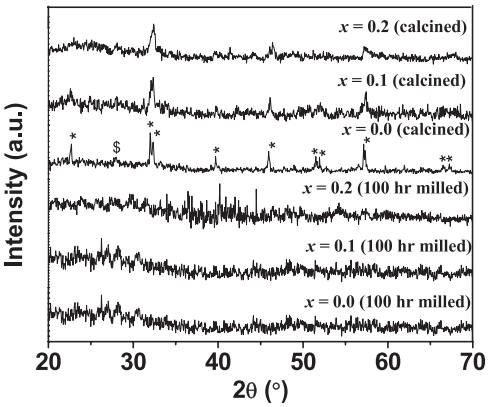

Figure 1. The room temperature XRD patterns of the $Bi_{1-x}Sm_xFeO_3$ compositions. ∗: $BiFeO_3$ (JCPDS 86-1518); $: suspected impurity phase.

3.2. Magnetization measurements

Figure 2 shows the room temperature magnetization (M) versus applied field (H) plots for all three samples with a maximum applied field of 1.75 T. One can see from this figure that the pure BFO sample possesses a very narrow hysteresis loop with a very small but nonzero remnant magnetization (M_r) of ∼8.56×10^{-4} emu g^{-1} and a coercive field (H_c) of ∼64.5 Oe. In an ideal BFO structure the net observed magnetization should be zero. Although the presence of the space modulated spin structure cancels the nonzero remnant magnetization (M_r) permitted by canted antiferromagnetic ordering, a small magnetization is observed. A possibility for the appearance of magnetization can be the presence of magnetic impurities. However in the present case the value of M_r is too small, showing that magnetic impurity phases as well as distorted spins, if present, are very small. On the other hand, BSFO-1 with $x = 0.1$ exhibits a much clearer hysteresis loop with higher M_r of ∼3.46×10^{-2} emu g^{-1} and H_c of ∼3250.12 Oe (see the inset in figure 2). The

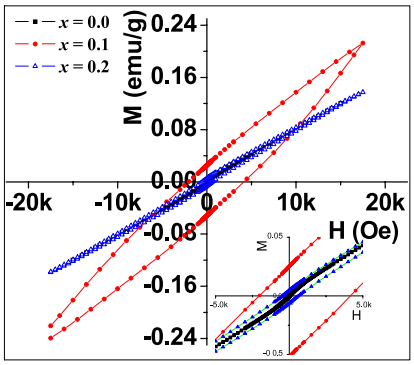

Figure 2. Room temperature magnetization versus applied magnetic field plots for $Bi_{1-x}Sm_xFeO_3$ samples. The inset shows a zoomed part near the origin.

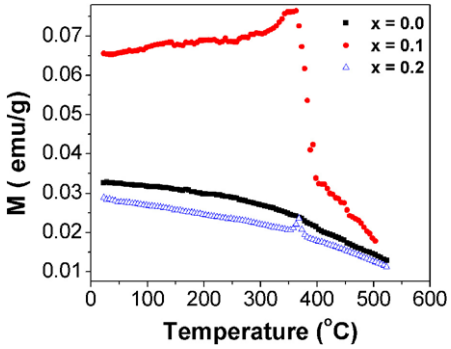

Figure 3. Magnetization versus temperature plots of $Bi_{1-x}Sm_xFeO_3$ compositions.

absolute value of M_r is still small but far above the sensitivity limit of the instrument. The coercive field H_c is indeed large and establishes beyond doubt loop opening on Sm doping. This increase in magnetization at 10 at.% Sm doping can be explained by the collapse of space modulated spin structure (to some extent) on Sm doping leading to a long-range canted antiferromagnetic order and possibly increased degree of canting [35, 36]. Another possibility that one can think of is again a magnetic impurity phase formation with 10% of Sm substitution. However, as shown later, further EPR and Mössbauer measurements do not support this. Upon further increasing the doping to 20 at.% Sm (BSFO-2), we obtained a rather narrower loop as compared to the BSFO-1 sample with M_r of $\sim 5.527 \times 10^{-3}$ emu g^{-1} and H_c of $\sim$535.52 Oe.

These observations suggest that while magnetization initially increases with Sm doping up to 10 at.%, it decreases on further increasing the Sm doping. The observed change in magnetic behaviour on increasing the doping is believed to happen due to further decrease in the extent of canting of spin structure, allowing a more perfect antiferromagnetic order. This aspect is further probed by electron paramagnetic resonance as shown in subsequent sections.

One can also observe that the M–H curve for BSFO-1 is not symmetric about the axes. As no such offset was observed in the case of the other two samples, the possibility of a residual field is remote. Such an offset can arise from the exchange interaction at the interfaces of ferromagnetic–antiferromagnetic components [37]. It is likely that the while most of the sample remains largely antiferromagnetic, regions in the Sm-doped BFO samples become weakly ferromagnetic and their interaction results in this offset.

Figure 3 shows the temperature dependence of the magnetization (M) of $Bi_{1-x}Sm_xFeO_3$ ($x = 0.0$, 0.1, 0.2) samples measured at 5 kOe. The plots show that the magnetization of undoped BFO decreases continuously with increase in the temperature, suggesting paramagnetic behaviour of the specimen, which is in contrast to the expected antiferromagnetic behaviour of the BFO samples. For the antiferromagnetic BFO, the ordering temperature is 643 K (370 °C). The absence of such a transition suggests that there are paramagnetic impurity phases in the BFO sample which could not be conclusively distinguished in the XRD results above the background fluctuation. This component did show up more clearly in Mössbauer spectroscopy as shown in later sections. On the other hand, doped samples, BSFO-1 and BSFO-2, show a magnetic transition at $\sim$370 °C, the same as the value of the Néel temperature for antiferromagnetic $BiFeO_3$. The BSFO-1 sample with 10 at.% Sm not only shows larger magnetization possibly for reasons explained above, but also exhibits a rather sharp transition as compared to the undoped sample at the known Néel temperature of pure BFO. This observation gives further evidence that the increased magnetization seen for BSFO-1 is not due to any impurity magnetic phase formed, but is due to the changes in the spin structure of the basic BFO configuration. The transition is rather less prominent in the case of BSFO-2 (20 at.% Sm doping) along with reduced magnetization, also suggested by the M–H measurements. To further explore the possible reasons for such behaviour, EPR and Mössbauer measurements were done and the results are shown in the following sections.

3.3. EPR measurements

To achieve a better understanding of the above magnetic behaviour, EPR measurements were carried out on the three samples. The first-derivative magnetic resonance absorption signals recorded at room temperature (RT) for three compositions BFO, BSFO-1 and BSFO-2 are shown in figures 4(a)–(c), respectively. The figures exhibit one intense signal with asymmetric line shape for each composition. There are three parameters which can be calculated from this figure which can be related to the magnetic structure of a solid: asymmetry parameter, P_{asy}; g-factor; and signal width ΔB_{p-p}. The asymmetry parameter P_{asy} is defined as $P_{asy} = (1 - h_U/h_L)$ where h_U is the height of the absorption peak above the base line and h_L is the height of the absorption peak below the base line of the first derivative of the magnetic resonance absorption signal. This parameter is an indication of the extent of the anisotropy in the magnetic structure of the sample. The g-factor is defined as $g = h\nu/\beta B_0$ where h is Planck's constant, β is the Bohr magneton, ν is the resonance frequency of the sample cavity and B_0 is the centre of the resonance absorption signal (the magnetic field where the baseline would cut the first-derivative signal).

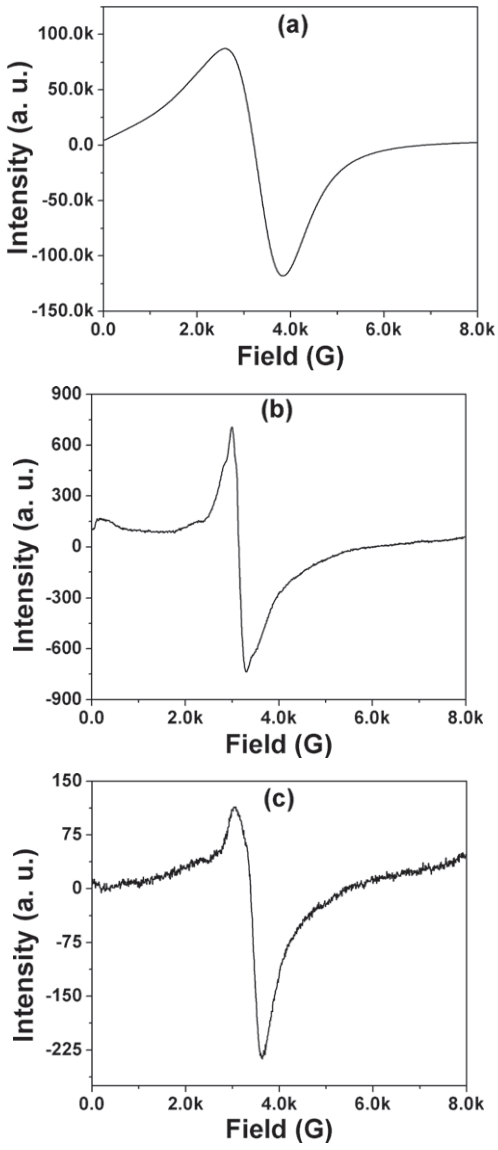

Figure 4. The room temperature EPR spectra of $Bi_{1-x}Sm_xFeO_3$ for (a) $x = 0.0$, (b) $x = 0.1$, (c) $x = 0.2$.

The centre of the EPR signal is represented in terms of the g-factor [38] and it can provide information about a paramagnetic centre's electronic structure. ΔB_{p-p} is the width of the signal defined as the separation between the upper peak and the lower peak. Calculated values of these parameters are shown in table 1. From table 1, it is seen that P_{asy} first decreases upon Sm doping and then increases on further Sm doping; similar behaviour is shown by the linewidth parameter. The g-factor also changes upon doping, showing a reverse trend. Due to the complex and heterogeneous magnetic nature of the samples, quantitative line shape analysis is difficult, but a qualitative explanation for the observations may be presented. The large value of P_{asy} for the pure BFO indicates a large magnetocrystalline anisotropy in the magnetic interactions. This anisotropy reduces upon Sm^{3+} doping. A fast magnetic exchange between magnetic moments of Sm^{3+} and Fe^{3+} would cause a narrowing of the linewidth as well as a reduction in shape anisotropy. Upon further increase of the

Table 1. Parameters of electron paramagnetic resonance spectra recorded at room temperature for various compositions of $Bi_{1-x}Sm_xFeO_3$.

Sample	g	$\Delta g/g$	$\Delta B_{p-p}(G)$	P_{asy}
BFO ($x = 0.0$)	2.187	0.093	1200	0.33
BSFO-1 ($x = 0.10$)	2.226	0.113	300	0.10
BSFO-2 ($x = 0.20$)	2.106	0.053	600	0.50

Sm^{3+} concentration, the magnetic dipolar interaction may start contributing to the linewidth resulting in a larger ΔB_{p-p} for the sample BSFO-2.

The degree of canting of spins is related to the g-value through the vector coefficient D whose magnitude is given by $D \approx (\Delta g/g)J_{super}$ where Δg is deviation of g from the value 2, i.e. $(g-2)$, and J_{super} is the superexchange interaction coefficient. As a rough approximation, assuming J_{super} to be constant for all samples, the value of D would be the largest for BSFO-1 as seen from $\Delta g/g$ values in table 1. This supports the VSM observations that the magnetic interactions are stronger in BSFO-1 as compared to the other two samples and one possible reason of the increased magnetization in BSFO-1 is the increased spin canting in this sample. However the change in magnetic characteristics between BSFO-1 and the other two samples seems to be much more than what the difference in value of D for these samples would indicate. It is likely that there could be sources other than spin canting for the enhanced magnetic character of the BSFO-1 sample. One reason could be differences in value of J_{super} for the three samples, depending upon the degree of exchange interaction. In addition, possibly Sm–Sm or Sm–Fe interaction manifests the magnetic structure in some way to give rise to the observed differences. The cycloidal spin structure could be only partially broken or broken only in parts of the sample which result in—albeit with a low absolute value—an increased M_r for the BSFO-1 sample.

3.4. Mössbauer spectroscopy

Figure 5 shows the Mössbauer spectra for BFO, BSFO-1 and BSFO-2 compositions, and table 2 shows various parameters extracted from these measurements. It is seen that while BSFO-1 and BSFO-2 samples show the presence of a single magnetically ordered phase, i.e. Sm-doped BFO characterized by a hyperfine magnetic field (B_{hf}) of ∼49 T, undoped BFO shows the presence of two other doublets which arise from a phase or phases which do not appear to be magnetically ordered. The total absorption area of the doublets is about 50%. The Mössbauer parameters of these doublets match closely with those of $Bi_2Fe_4O_9$ [29]. This compound consists of Fe^{3+} ions distributed almost equally in approximately octahedral and tetrahedral coordinations and the two doublets in the Mössbauer spectra correspond to these two environments. The two doublets in pure $Bi_2Fe_4O_9$ have quadruple splits of 0.84 and 0.42 mm s^{-1} [29, 39], close to what we have observed. While the spectrum of the undoped BFO sample shows a clear doublet structure corresponding to the impurity $Bi_2Fe_4O_9$ phase, the spectra for BSFO-1 and BSFO-2 do not show any

Table 2. Hyperfine parameters obtained from Mössbauer spectra; δ—isomer shift, ΔE_Q—quadrupole splitting, Γ—linewidth, B_{hf}—magnetic hyperfine field, A—subspectral area.

Sample	δ (mm s^{-1})	ΔE_Q (mm s^{-1})	Γ (mm s^{-1})	B_{hf} (T)	A (%)
BFO ($x = 0.0$)	0.12	0.79	0.27	—	26
	0.41	0.56	0.26	—	23
	0.38	0.09	0.46	49.3	51
BSFO-1 ($x = 0.10$)	0.39	−0.02	0.38	49.5	100
BSFO-2 ($x = 0.20$)	0.38	−0.06	0.42	49.1	100

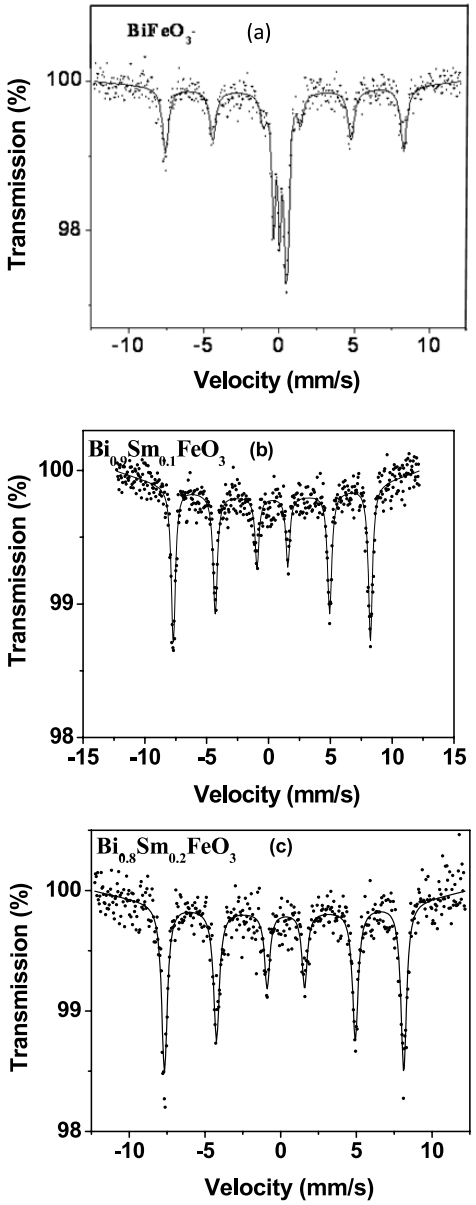

Figure 5. Mössbauer spectra of $Bi_{1-x}Sm_xFeO_3$ for (a) $x = 0.0$, (b) $x = 0.1$, (c) $x = 0.2$.

such component. The same synthesis procedure with 10 at.% and 20 at.% Sm gives a perfect single sextet showing that only Sm-doped perovskite structured BFO phase is formed. This supports our assertion that the increased magnetization in BSFO-1 is due not to impurity phase but to the change in magnetic interaction caused by Sm substitution in the BFO lattice. Mössbauer results for undoped BFO are in contrast to the XRD results where secondary phases are not clearly observed, especially for the undoped BFO sample, and their relative abundances could not be ascertained for these samples. This also highlights the importance of Mössbauer spectroscopy in unravelling the phases at atomic resolution.

4. Conclusions

$Bi_{1-x}Sm_xFeO_3$ ceramic samples were synthesized at relatively low calcination temperatures by a mechanical activation assisted solid-state-reaction method. While undoped samples show negligible remnant magnetization, the samples doped with Sm at $x = 0.1$ show significantly higher remnant magnetization and coercive field as well as a sharp magnetic transition at ∼370 °C, which is the same as the characteristic Néel temperature of pure antiferromagnetic BFO. Increase in the doping level to $x = 0.2$ leads to a drop in the magnetization although a magnetic transition is still observed. Mössbauer spectroscopy confirms the single-phase nature of Sm-doped samples whilst the presence of secondary phases is confirmed in the case of the undoped sample. The increase in the magnetization is accompanied by an increased degree of spin canting as suggested by the narrowing of the line in the EPR spectra for $x = 0.1$, which further increases the line broadening (i.e. decreased spin canting) at $x = 0.2$. The improvement in the magnetic properties at $x = 0.1$ are likely to be caused by a combination of factors such as the propensity of the sample towards pure perovskite phase formation, partial destruction of spin cycloids, increased degree of canting and magnetic interactions between magnetic ions, namely Fe and Sm.

Acknowledgments

One of the authors (AG) thanks the Department of Science and Technology (DST) New Delhi, Government of India, for financial support for this research.

References

[1] Eerenstein W, Mathur N D and Scott J F 2006 *Nature* **442** 759–65
[2] Van Aken B B, Rivera J-P, Schmid H and Fiebig M 2007 *Nature* **449** 702–5
[3] Fiebig M 2005 *J. Phys. D: Appl. Phys.* **38** R123–52
[4] Smolenskii G A and Chupis I E 1982 *Sov. Phys.—Usp.* **25** 475–93

[5] Danilkevitch M I and Makoed I I 2000 *Phys. Status Solidi* **222** 541–51
[6] Venevtsev Yu N, Zhdanov G S and Solov'ev S P 1960 *Sov. Phys.—Crystallogr.* **4** 538–40
[7] Smolenskii G A, Isupov V A, Agranovskaya A I and Krainik N N 1961 *Sov. Phys.—Solid State* **2** 2651–4
[8] Michel C, Moreau J-M, Achenbach G D, Gerson R and James W J 1969 *Solid State Commun.* **7** 701–4
[9] Moreau J-M, Michel C, Gerson R and James W J 1971 *J. Phys. Chem. Solids* **32** 1315–20
[10] Sosnowska I, Peterlin-Neumaier T and Steichele E 1982 *J. Phys. C: Solid State Phys.* **15** 4835–46
[11] Kadomtseva A M, Zvezdin A K, Popov Yu F, Pyatakov A P and Vorob'ev G P 2006 *JETP Lett.* **79** 571–81
[12] Kanai T, Ohkoshi S-I, Nakajima A, Watanabe T and Hashimoto K 2001 *Adv. Mater.* **13** 487–90
[13] Béa H, Bibes M, Petit S, Kreisel J and Barthelemy A 2007 *Phil. Mag. Lett.* **87** 165–74
[14] Gabbasova Z V, Kuz'min M D, Zvezdin A K, Dubenko I S, Murashov V A, Rakov D N and Krynetsky I B 1991 *Phys. Lett.* A **158** 491–8
[15] Fedulov S A, Ladyzhinskii P B, Pyatigorskaya I L and Venevtsev Y N 1964 *Sov. Phys.—Solid State* **6** 375–8
[16] Kumar M M, Srinath S, Kumar G S and Suryanarayana S V 1998 *J. Magn. Magn. Mater.* **188** 203–12
[17] Yuan G L and Or S W 2006 *J. Appl. Phys.* **100** 024109
[18] Nalwa K S and Garg A 2008 *J. Appl. Phys.* **103** 044101
[19] Liu Y-P and Wu J-M 2007 *Electrochem. Solid State Lett.* **10** G39–41
[20] Vasudevan S, Rao C N R, Umarji A M and Rao G V S 1979 *Mater. Res. Bull.* **14** 451–4
[21] Sosnowska I, Schafer W and Troyanchuk I O 2000 *Physica* B **276** 576–7
[22] Takahashi K and Tonouchi M 2007 *J. Magn. Magn. Mater.* **310** 1174–6
[23] Azuma M, Kanda H, Belik A A, Shimakawa Y and Takano M 2007 *J. Magn. Magn. Mater.* **310** 1177–9
[24] Jun Y-K and Hong S-H 2007 *Solid State Commun.* **144** 329–33
[25] Li M, Ning M, Ma Y, Wu Q and Ong C K 2007 *J. Phys. D: Appl. Phys.* **40** 1603–7
[26] Kothari D, Reddy V R, Sathe V G, Gupta A, Banerjee A and Awasthi A M 2008 *J. Magn. Magn. Mater.* **320** 548–52
[27] Lebeugle D, Colson D, Forget A, Viret M, Bonville P, Marucco J F and Fusil S 2007 *Phys. Rev.* B **76** 024116
[28] Radaev S F, Muradyan L A and Simonov V I 1991 *Acta Crystallogr.* B **47** 1–6
[29] Kostiner E and Shoemaker G L 1971 *J. Solid State Chem.* **3** L186–9
[30] Duran-Martin P, Castro A, Millan P and Jimenez B 1998 *J. Mater. Res* **13** 2565–71
[31] Xue J M, Wang J and Rao T M 2001 *J. Am. Ceram. Soc.* **84** 660–2
[32] Wang J, Wan D M, Xue J M and Ng W B 1999 *J. Am. Ceram. Soc.* **82** 477–9
[33] Wang J, Xue J M, Wan D M and Gan B K 2000 *J. Solid State Chem.* **154** 321–8
[34] Gu H, Zhang T, Cao W, Xue J M and Wang J 2003 *Mater. Sci. Eng.* B **99** 116–20
[35] Zalesskii A V, Frolov A A, Khimich T A and Bush A A 2003 *Phys. Solid State* **45** 141–5
[36] Lee Y H, Wu J M and Lai C H 2006 *Appl. Phys. Lett.* **88** 042903
[37] Meiklejohn W H and Bean C P 1957 *Phys. Rev.* **105** 904–13
[38] Chand P, Srivastava R C and Upadhyay A 2008 *J. Alloys Compounds* **460** 108–14
[39] Bokov V A, Novikov G V, Trukhtanov V A and Yushchuk S I 1970 *Sov. Phys.—Solid State* **II** 2324–6